Hindawi Publishing Corporation
Indian Journal of Materials Science
Volume 2015, Article ID 196178, 12 pages
http://dx.doi.org/10.1155/2015/196178

Research Article

Mechanical Characterization and Machinability Behavior of Annealed AISI D6 Cold Working Steel

Manoj Nayak, Rakesh Sehgal, and Rajiv Kumar Sharma

Department of Mechanical Engineering, National Institute of Technology, Hamirpur 177005, India

Correspondence should be addressed to Manoj Nayak; manojnayak69@gmail.com

Received 15 May 2015; Accepted 18 August 2015

Academic Editor: Jose L. Endrino

Tool steels in metal forming industry are exposed to complex and aggressive conditions due to multiple effects (mechanical, thermal, or tribological loading) and require defined mechanical properties. Also machining of tool steel with poor machinability like AISI D6 to manufacture form tools is an extremely difficult task. This paper investigates the microstructural, mechanical, and machining behavior of AISI D6 steel in annealed and hardened conditions. Various mechanical tests indicated good hardenability, improved surface hardness, and phenomenal improvement in tensile strength but extremely poor resistance to impact in both annealed and hardened condition for this steel. The machining characteristics of AISI D6 steel were evaluated using a 2^k unreplicated full factorial design approach and statistical techniques have been used to assess and identify the significant factors, namely, cutting speed, feed, depth of cut, and approach angle, in minimizing surface roughness and main cutting force while machining this steel with a carbide tool. It was found that the depth of cut, feed, and approach angle are the most significant factors affecting the surface roughness and depth of cut and feed affect the main cutting force. Cutting speed has no effect on surface roughness and main cutting force in machining of the steel in annealed condition.

1. Introduction

Tool steels for drawing dies, cold extrusion dies, broaches, mandrels, tooling for compaction of steel powder, thread rolls, burnishing rolls, and forming rolls should have good mechanical properties, exhibit minimal distortion on hardening, and provide good machinability. Metal forming processes such as cold forging, cold deep drawing, thread rolling, or any form of rolling are performed using high strength tool steels. Apart from high resistance to wear, dynamic loading, thermal shocks, and fracture, these steels own a high tensile and compression yield strength to resist plastic deformations at localized stress concentration points in the tooling. Hence well-defined mechanical and tribological properties of the material are required to limit the high cost of wear to metal forming industry incurred due to the complex and demanding phenomenon [1].

Tool steel for cold work includes three classes of steel with AISI designation O, A, and D. Each of these classes has high carbon content for high hardness and high wear resistance in cold working applications but differs in alloy content, which affects the hardenability and the carbide distributions incorporated in the hardened microstructure. AISI D6 is high carbon high chromium steel containing carbon 2.00–2.50%. It is further modified to obtain better machinability and less brittleness by lowering the carbon content to 1.00–1.50% and is commercially available as AISI D1, D2, D3, D4, and D5 steel. Good steel machinability is defined as a combination of low power consumption, low tool wear, and good surface finish [2]. These steels should be easily machinable in annealed condition. Steel mills provide the tool steel in the annealed condition so that the machinist can readily machine the tool steel into a premachined tool providing machining allowances. Poor surface finish, high cutting force, and high tool wear are also observed during machining of tool steels. Surface quality generated and machining performance of the tool steels are determined by cutting parameters, types of coolants, types of tool material, and tool coating used during machining.

Podgornik et al. [1] in their experimental study found that cryogenic treatment to tool steels improves dimensional stability, abrasive, fatigue, and wear resistance and increases

strength and hardness of the material. Amini et al. [3] studied the effects of cryogenic treatment on the wear behavior of AISI D6 tool steel using a pin-on-disk wear tester. The material demonstrated improved wear resistance and hardness due to more homogenized carbide distribution as well as the elimination of the retained austenite compared with the shallow cryogenic treatment. Further improvement in wear resistance and hardness was achieved by keeping the samples for a period of one week at room temperature after quenching (stabilization) as more retained austenite was transformed into martensite. Naravade et al. [4] studied the wear behaviors of AISI D6 tool steel after cryogenic treatment, which showed decreased retained austenite and thereby improvement in wear resistance and hardness. Bressan et al. [5] carried out an experiment to evaluate the mechanical properties of AISI D6 steel in heat treated and in annealed condition. Their results showed an increase in yield stress by 40% and decrease in toughness by 50% after heat treatment.

Davim and Figueira [6] experimentally investigated the machinability of AISI D2 tool steel to find the significant factors. The feed rate and cutting time, which, respectively, showed contribution of 29.6% and 32% using statistical techniques, were the most significant factors. Cakir et al. [7] developed mathematical models for predicting the surface roughness of AISI P20 cold work tool steel in annealed condition using two types of inserts. They suggested that, among the cutting parameters, feed rate has the greatest significance and depth of cut the least and observed poor surface finish with higher feed rate and good surface finish with high cutting speed. Fnides et al. [8] in an experimental study developed statistical models for cutting forces in hard turning of AISI H11 hot work tool steel showing depth of cut as the dominant factor instead of feed rate. Bouacha et al. [9] used statistical analysis to find the most significant factors during machining of hardened AISI 52100 material using CBN tools. They found that the surface roughness is influenced by feed rate and cutting speed, main cutting forces are influenced by depth of cut, and thrust forces are sensitive to workpiece hardness and negative rake angle. Lima et al. [10] in an experimental study observed good surface finish while turning a softer steel AISI 4340 steel using low feed rates and depths of cut and improved surface finish at high cutting speed. Lalwani et al. [11] investigated the influence of cutting conditions like cutting speed, feed rate, and depth of cut on cutting forces and surface roughness during hard turning of MDN250 steel using coated ceramic tool and showed that when cutting speed and depth of cut are at high level and feed is at low level, good surface finish is achieved. Ebrahimi and Moshksar [12] observed poor machinability during machining of microalloyed steel (30MnVS6) and quenched tempered (QT) steels (AISI 1045 and AISI 5140), at different cutting conditions (depth of cut was kept constant, feed rate was in range of 0.11, 0.22, and 0.44 mm/rev., cutting speed was 10–250 m/min, and hardness was of 245 and 330 BHN). These studies suggest that machining characteristics of hardened and annealed steel are different and have different significant factors influencing different quality characteristics.

The cost of wear to metal forming industry due to complex and demanding mechanical, thermal, chemical, or tribological loading is so high that it requires well-defined mechanical and tribological properties along with continuing development in the field of advanced materials. The concern is of good uniform machinability of tool steels as the cost of machining accounts for a large amount of total cost of tools, moulds, and dies. Otherwise grinding equipment and practices used for tool steels with CBN wheel for the best performance become costlier. Literature survey reveals that only a few studies have been done in evaluating the mechanical and machining behaviour of AISI D6 tool and hence the present study focuses on mechanical and machinability aspects of the tool steel.

2. Material and Methods

2.1. Metallurgical Test. The material was subjected to metallurgical test according to ASTM E 415 [13] on an Emission Spectrometer, Make: LECO, USA, Model GDS500A. The chemical composition of test material is C 2.130%; Si 0.238%; Mn 0.240%; Cr 11.10%; Ni 0.090%; Mo 0.032%; V 0.130%; Cu 0.030%; Al 0.06%; S 0.02%; P 0.010%; Co 0.025%; W 0.620%; Fe 85.267%. The test material conforms to ASTM A 681 standard of ASM Handbook (Vol. 1) [14]. The carbon content of the steel influences the martensitic hardening and 2.130% of carbon present in this steel is an advantage. Traces of other alloying elements are seen apart from the prominent presence of chromium and tungsten because on austenitizing some of the carbide dissolves in the austenite, thus supplying the matrix with alloying elements necessary for high hardenability and as quenched hardness. The steel is alloyed with Cr, W to get hard and abrasive resistance carbides in the steel. The hard carbides in steel reduce the machinability by giving a high wear on the cutting tool. The presence of tungsten in this steel produces very high densities of stable carbides. The presence of high chromium content enables this steel to resist staining particularly form tools when the steel is hardened and polished. The presence of vanadium benefits the effects of mechanical properties and refines austenite grain size.

2.2. Hardness Measurement. The hardness of the steel measured according to BIS, IS: 1586-2000 [15], in annealed condition was 96.8 HRB and 58 HRC after hardening and tempering. On each specimen several measurements were performed across the surface in order to obtain representative average hardness value.

2.3. Microhardness Measurement. A Vickers hardness testing machine capable of applying a predetermined force with the required range of test forces, an indenter and measuring device, was used to measure the surface hardness of the test piece. The test piece of Ø 42 × 12 mm cylindrical work pieces was faced on the flat face with CBN tool (cutting condition 775 rpm; DOC = 0.1 mm; feed 0.1 mm/rev.) to generate a surface. The Rockwell hardness measured on the surface of the steel according to BIS, IS: 1586-2000 [15], was 59.7 HRC. The Vickers hardness test was conducted in accordance to BIS, IS: 1501-2002 [16], and the test forces along with the results are shown in Table 1. The approximate hardness ranges

Table 1: Microhardness of the steel.

Serial number	9807 N for 15 sec	4903 N for 15 sec	2942 N for 15 sec
1	788.6	828.6	798.2
2	796.7	843.3	806.3
3	785.1	815.1	802.5
4	791.0	844.7	797.7
Average	790 HV1	833 HV0.5	801 HV0.3

between 63 and 64 HRC which only suggests the increase of hardness on the surface as a result of metallurgical alteration due to the cutting forces and temperature. This hardened surface further improves the wear and abrasion resistance of the tool surface and prevents any hard particles usually leaving deep scratches and causing damage to the form rolls.

2.4. Hardenability Test. The hardness measured on the surface after hardening and tempering of the steel according to IS: 1586-2000 was 60.3 HRC [15]. To measure the hardness of the steel at the core, step turning procedure was adopted. The hardness values were taken in each step turned at 5 mm below the surfaces generated. It was found that there was hardly any major variation of hardness at the surface of Ø 42 mm and at Ø 15 mm core of the cylinder. The hardness varied from 59.3 HRC at the surface to 57.8 HRC at the core. This only suggests that the material is very much susceptible to through hardening and possesses good hardenability property.

2.5. Optical Microscopic Test. Optical microscopic test was done using an inverted optical microscope as per ASME standard. The two test samples, one before heat treatment and one after heat treatment, were sectioned from two lengths (one length each from hardened and nonhardened lengths) with an abrasive cutter and then polished successfully with emery paper with fine grit meshes 120, 320, 400, 600, and 2000 followed by polishing with velvet cloth using diamond paste and diamond fluid until mirror like surface was obtained. The samples were then cleaned using lab detergent and immediately rinsed using running water and then dried using hot air immediately followed by etching to prevent surface oxidation using 3% nital solution (3 mL of HNO_3 and 97% methanol) and the observation was done under the optical microscope.

The microstructure observed in the annealed steel is of massive and spheroidal carbides in ferrite matrix as shown in Figure 1 and long granular carbides in tempered martensite as shown in Figure 2. The presence of chromium carbides in the ferrite matrix is clearly noted. Dispersion of small and large particles is seen in both of the conditions. The only disadvantage of the steel is that the long granular carbide dendrites as seen in the hardened steel are brittle and if found on the machined surface of the dies and rolls are prone to chipping and fracture.

2.6. Tensile Test. Tensile test was performed according to BIS, IS: 1608-2005 [17], on a 40-tonne UTM. Tool steel bars

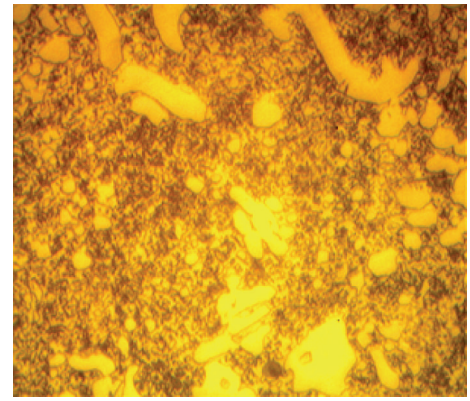

Figure 1: Micrographs in annealed state.

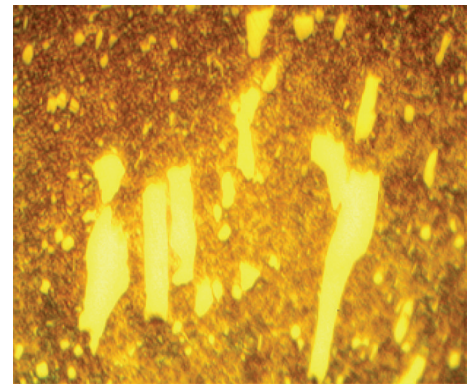

Figure 2: Micrographs after heat treatment.

Table 2: Tensile test data.

Parameter	Specimen 1 (annealed)	Specimen 2 (hardened and double tempered)
Hardness measured	98.6 HRB	58 HRC
Diameter (mm)	10.00	10.02
Area (mm^2)	78.50	81.67
Gauge length (mm)	50.00	50.00
Breaking load (N)	54000	151500
Yield load (N)	35000	No yield
Elongated length (mm)	53.70	50.58
Tensile strength (mm)	687.90	1855.03
Yield stress (N/mm^2)	445.86	NA
Elongation %	7.40	1.16

were machined to a smooth gage section in the center and a larger shoulder on each end for tensile tests. For each test condition two samples were tested and average value was reported as given in Table 2. The tensile strength of tool steel is directly related to its hardness. The hardness of the tensile specimen was measured to be 57 HRC. The tensile strength of the hardened steel improved phenomenally from 687.90 to 1855.03 N/mm^2 and the ductility decreased from 7.40 to 1.16% (Table 2). Although compressive yield strength is of more

Table 3: Charpy (V-notch) impact test data.

Serial number	Absorbed energy for annealed specimen in KV	Absorbed energy for hardened specimen in KV with double tempering
1	4 J	3 J
2	4 J	3 J
3	4 J	3 J
Average	4 J	3 J

importance but tensile strength and ductility are important properties in tooling area as in some situations a preexisting crack in tools starts developing due to tension. No yielding phenomenon was observed in the hardened specimen and fracture occurred without any prior yield. The yield strength of the annealed steel was 445.69 N/mm^2 and brittle cleavage was observed on all of the fractured surfaces.

2.7. Charpy (V-Notch) Test. Characterization of the toughness is done by this test. This test specifies the Charpy impact (V-notch) method for determining impact strength of the tested steel and was conducted as per BIS, IS: 1757-1988 [18]. Nine standard steel specimens or three sets (three specimens in each set) for this experiment were machined from annealed steel bar. Two sets of the steel specimens were hardened and one set was tempered twice and another set was tempered thrice and the average Rockwell hardness was measured to be 55 ± 2 HRC and then subjected to Charpy impact test.

The test piece was made to lay squarely against the supports, with the plane on symmetry of the notch within 0.5 mm of the plane midway between them. It was made to strike by the striker in the plane of the symmetry of the notch and on the side opposite the notch. The results are shown in Table 3. The results indicate that the material has a very poor resistance to impact in both annealed and hardened condition. Brittleness is characterized by fracturing with low energy under impact. Characteristics of cleavage and brittleness were observed with fine grained fracture surface.

2.8. Machinability Test

2.8.1. Work and Tool Material. Annealed cold working tool steel AISI D6 with 96.8 HRB was selected for this machinability study using cemented carbide inserts. CVD coated (multiphase Al_2O_3) carbide inserts bearing ISO code CCMT 09T308N-SU with 80° rhombus shape, having cutting geometry 6° rake angle, 7° relief angle, and 0.793 mm nose radius, were used.

2.8.2. Machine and Equipment Used. The experiments were carried out on an all geared DRO Lathe (Model: Bajaj-Pioneer-175 Geared Headed), 8-spindle cutting speed (8–1200 rpm), and 24 numbers of feeds as shown in Figure 3. A dynamometer (Make TELC Germany) with quick approach/feed angle adjustment 45°, 60°, 75°, and 90° CCMT09 tool seat in the tool holder with XKM 2000 software was used for cutting force and temperature measurements. A surface roughness tester (SJ-301 Mitutoyo, Japan), x-axis (drive units), with measuring range of 12.5 μm was used to measure the surface roughness (R_a) during the experiments.

Figure 3: Cutting force measurement.

2.8.3. Experimental Procedure. The samples of both the annealed and hardened workpiece were machined by removing 0.5 mm thickness of the top cylindrical surface to Ø 41 × 150 mm, in order to eliminate any surface defects and wobbling and then centered and faced. Tests were performed to identify the main effects of machining parameters on surface roughness and cutting forces. The independent variables are cutting speed, feed, depth of cut, and approach angles for annealed workpiece and the independent variables are cutting speed, feed, depth of cut, and workpiece hardness for hardened steel. Corresponding cutting speeds were equalized at different workpiece diameters to the extent that rotational speed ratios permit. Short duration tests were performed (machined length of 20 mm) without coolant. Each test was realized with fresh cutting edge.

Surface roughness was measured offline with the profilometer by taking the measurements across the lay. Three measurements (λ_c = 0.8 mm; N = 5) were taken along the feed length for each sample length machined and measurements were made about 120° apart and the average value was used in the analysis. The cutting force and its components generated on the tool point in the turning operation were measured using a lathe tool dynamometer (Make DKM 2010 of TELC Germany) with software XKM 2000 as shown in Figure 3. In the present work, the machining process of the annealed steel was studied under DOE with full factorial unreplicated design (2^4) giving all combinations of factors at two levels as shown in Table 4 and sixteen experimental runs were taken and 50% of the experiments were repeated to minimize the experimental error. The two levels of these parameters have been decided on the basis of literature review, machine capabilities, and shop floor practice and the experiments were conducted randomly and measurements are shown in Table 5.

Table 4: Experimental factors and factor levels for annealed steel.

Code	Process parameters	Low level	High level
A	Cutting speed (V)	39.6	97.5
B	Feed (f)	0.1	0.27
C	Depth of cut (d)	0.2	1.0
D	Approach angle (A_e)	45	90

Table 5: Matrix design and experimental data.

Std.	Run	V (m/min)	"f" (mm)	"d" (mm)	A_e (degree)	R_a (μm)	F_c (N)
3	1	39.6	0.27	0.2	45	2.78	349
2	2	97.5	0.10	0.2	45	0.76	164
13	3	39.6	0.10	1.0	90	4.18	461
11	4	39.6	0.27	0.2	90	3.35	170
4	5	97.5	0.27	0.2	45	3.22	298
6	6	97.5	0.10	1.0	45	2.76	412
1	7	39.6	0.10	0.2	45	0.96	188
15	8	39.6	0.27	1.0	90	4.09	871
10	9	97.5	0.10	0.2	90	0.71	108
14	10	97.5	0.10	1.0	90	4.91	408
7	11	39.6	0.27	1.0	45	3.08	614
12	12	97.5	0.27	0.2	90	2.90	189
5	13	39.6	0.10	1.0	45	3.28	307
8	14	97.5	0.27	1.0	45	1.07	722
9	15	39.6	0.10	0.2	90	1.06	132
16	16	97.5	0.27	1.0	90	3.11	747

3. Results and Discussion

The results and discussion for determining the significant factors using statistical analysis during machining of the steel in annealed condition are presented in the following subsections.

3.1. Statistical Analysis. The two-level statistical design for four independent variables consists of sixteen factorial points ($2^4 = 16$) where each variable is fixed at two levels. The surface roughness and main cutting force are assumed to be linearly dependent on the level of each independent factor. The effect of each experimental factor can be defined as the change in the response when the factor changes from one level to another level such as from high to low. An interaction is the variation among the differences between means for different levels of one factor over different levels of the other. MINITAB-15 is used in this analysis process, with an approach to the statistical analysis of the 2^k design as discussed by Montogomery [19].

3.1.1. Estimating the Factor Effects. In a single replicate of 2^k there is no internal estimate of error. The approach to the analysis of an unreplicated factorial is to assume that certain high order interactions are negligible and combine their mean squares to estimate the error. A simple method of analysis suggested is to examine a normal probability plot of the estimates of the effects. This is a plot of the absolute value of the effect estimates against their normal probability. Here the effects which are active and real will have nonzero mean and will fall off the straight line, whereas the inactive and insignificant effects that are normally distributed, with zero mean and variance σ^2, will fall along the straight line. The graphs in Figures 4 and 5 suggest that the assumption of normal distribution is fairly reasonable; factors f, d and interaction of $f \times d$, $d \times A_e$ are statistically significant for main cutting force; factors d *and* A_e and interaction of $f \times d$, are statistically significant for surface finish. Since $f \times d$ lie on the left hand side of the line, their contribution has negative effect on the model. The reverse is true for the rest of the significant effects lying on right hand side. The estimated effect and coefficient for surface roughness and main cutting force are shown in Tables 6 and 7. Analysis of variance (ANOVA) is carried out to test the null hypothesis that the main effect and

Table 6: Estimated effects and coefficients for surface roughness (coded units).

Term	Effect	Coef.	SE coef.	T	p
Constant		2.6387	0.1432	18.43	0.000
V	−0.4175	−0.2087	0.1432	−1.46	0.205
f	0.6225	0.3113	0.1432	2.17	0.082
d	1.3425	0.6713	0.1432	4.69	0.005
A_e	0.8000	0.4000	0.1432	2.79	0.038
$V \times f$	−0.3325	−0.1662	0.1432	−1.16	0.298
$V \times d$	−0.2775	−0.1388	0.1432	−0.97	0.377
$V \times A_e$	0.1550	0.0775	0.1432	0.54	0.612
$f \times d$	−1.5675	−0.7838	0.1432	−5.47	0.003
$f \times A_e$	0.0250	0.0125	0.1432	0.09	0.934
$d \times A_e$	0.7250	0.3625	0.1432	2.53	0.052

S = 0.572735, PRESS = 16.7949, and R-Sq = 93.80%.
R-Sq (pred.) = 36.47%, R-Sq (adj.) = 81.39%.

Table 7: Estimated effects and coefficients for main cutting force (coded units).

Term	Effect	Coef.	SE coef.	T	p
Constant		384.25	15.78	24.35	0.000
V	−6.50	−3.25	15.78	−0.21	0.845
f	223.50	111.75	15.78	7.08	0.001
d	367.00	183.50	15.78	11.63	0.000
A_e	5.00	2.50	15.78	0.16	0.880
$V \times f$	−7.50	−3.75	15.78	−0.24	0.822
$V \times d$	15.50	7.75	15.78	0.49	0.644
$V \times A_e$	−41.00	−20.50	15.78	−1.30	0.251
$f \times d$	118.00	59.00	15.78	3.74	0.013
$f \times A_e$	−4.50	−2.25	15.78	−0.14	0.892
$d \times A_e$	103.00	51.50	15.78	3.26	0.022

S = *63.1189*; PRESS = 203981.
R-Sq = *97.70*%, R-Sq (pred.) = 76.42%, and R-Sq (adj.) = *93.09*%.

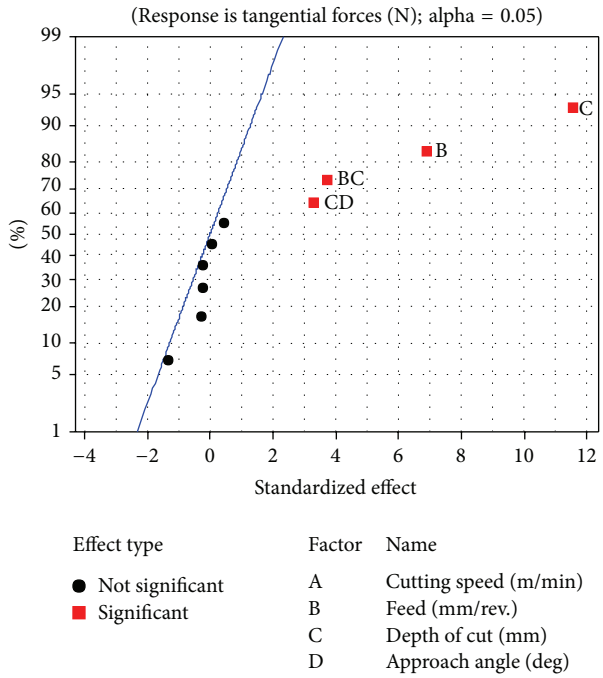

Figure 4: Normal plot of the standardized effects (F_c).

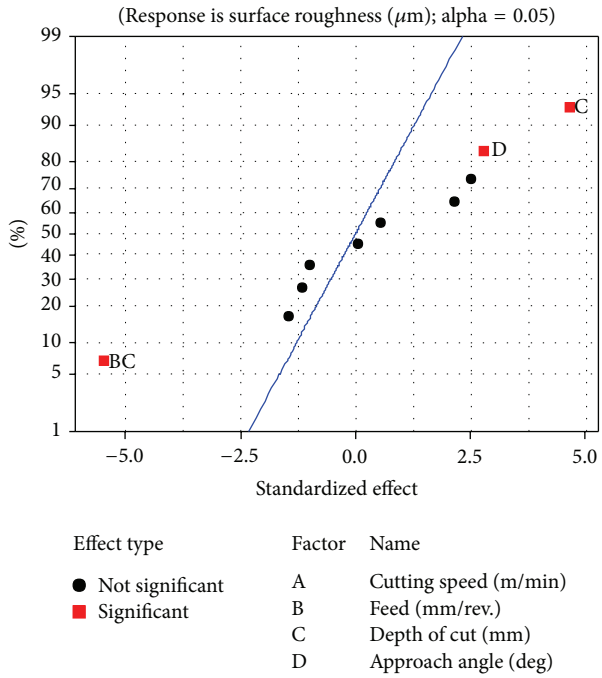

Figure 5: Normal plot of the standardized effects (R_a).

the interactions are equal to zero. The small p values (<0.05) mean that all the main effects and interactions are zero at the 5% significance level. In other words, there is reasonably strong evidence that at least some of the main effects and interactions are not equal to zero.

Table 8: ANOVA for surface roughness.

Source	DF	Seq. SS	Adj. SS	Adj. MS	F	p
V	1	0.6972	0.6972	0.6972	2.13	0.205
f	1	1.5500	1.5500	1.5500	4.73	0.082
d	1	7.2092	7.2092	7.2092	21.98	0.005
A_e	1	2.5600	2.5600	2.5600	7.80	0.038
$V \times f$	1	0.4422	0.4422	0.4422	1.35	0.298
$V \times d$	1	0.3080	0.3080	0.3080	0.94	0.377
$V \times A_e$	1	0.0961	0.0961	0.0961	0.29	0.612
$f \times d$	1	9.8282	9.8282	9.8282	29.96	0.003
$f \times A_e$	1	0.0025	0.0025	0.0025	0.01	0.934
$d \times A_e$	1	2.1025	2.1025	2.1025	6.41	0.052
Error	5	1.6401	1.6401	0.3280		
Total	15	26.4362				

$S = 0.572735$, R-Sq = 93.80%, and R-Sq (adj.) = 81.39%.

3.1.2. Initial Model

Surface Roughness. The regression model equation for surface roughness is represented by

$$\begin{aligned} R_a = {} & 2.639 - 0.21x_1 + 0.311x_2 + 0.671x_3 + 0.4x_4 \\ & - 1.66x_1x_2 - 0.139x_1x_3 + 0.0.077x_1x_4 \\ & - 0.784x_2x_3 + 0.012x_2x_4 + 0.3625x_3x_4 + \cdots \\ & + \varepsilon, \end{aligned} \quad (1)$$

where factors A, B, C, and D are represented by x_1, x_2, x_3, and x_4.

Main Cutting Force. The regression model equation for main cutting force is represented by

$$\begin{aligned} F_c = {} & 384.25 - 3.25x_1 + 111.75x_2 + 183.5x_3 + 2.50x_4 \\ & - 3.75x_1x_2 + 7.75x_1x_3 - 20.50x_1x_4 + 59.00x_2x_3 \\ & - 2.25x_2x_4 + 51.50x_3x_4 + \cdots + \varepsilon. \end{aligned} \quad (2)$$

3.1.3. Statistical Testing. The main effects are highly significant (those having small p value); p value indicates that the two main factors "d" and "A_e" and the interaction $f \times d$ have statistically significant effect on the surface roughness. The ANOVA for main cutting force shows the main effects which are highly significant (all having small p value); p value indicates that the two main factors "f" and "d" and their interactions have statistically significant effect on the response. The ANOVA in Tables 8 and 9 indicates the specific effects and interaction, which are statistically significant or insignificant.

3.1.4. Refining of Model. Refining the model usually consists of removing of any nonsignificant variables from the full

Table 9: ANOVA for main cutting force.

Source	DF	Seq. SS	Adj. SS	Adj. MS	F	p
V	1	169	169	169	0.04	0.845
f	1	199809	199809	199809	50.15	0.001
d	1	538756	538756	538756	135.23	0.000
A_e	1	100	100	100	0.03	0.880
$V \times f$	1	225	225	225	0.06	0.822
$V \times d$	1	961	961	961	0.24	0.644
$V \times A_e$	1	6724	6724	6724	1.69	0.251
$f \times d$	1	55696	55696	55696	13.98	0.013
$f \times A_e$	1	81	81	81	0.02	0.892
$d \times A_e$	1	42436	42436	42436	10.65	0.022
Error	5	19920	19920	3984		
Total	15	864877				

$S = 63.1189$, R-Sq = 97.70%, and R-Sq (adj.) = 93.09%.

model. Thus the final regression model for surface finish is represented by

$$R_a = 2.639 + 0.671x_3 + 0.4x_4 - 0.784x_2x_3. \quad (3)$$

The final regression model for main cutting force is represented by

$$F_c = 384.25 - 111.75x_2 + 183.5x_3 + 59.00x_2x_3 + 51.50x_3x_4. \quad (4)$$

3.1.5. Residual Analysis. Regression modeling is done to obtain the predicted or fitted value of the response surface finish (R_a) only. Similar analysis can be done for main cutting force. Violation of the basic assumptions and model adequacy can be easily investigated by the examination of residuals. Residual plots are frequently used to diagnose inequality of variance. These are discussed in the following subsections.

(i) Normal Probability Plot. Normal probability plot of the raw data is used to check the assumption of normality when using the t-test. The equal variance and normality assumptions are easy to check using a normal probability plot. It indicates whether the data are normally distributed, other variables are influencing the response, or outlier exists in the data. It can be seen from Figure 6 that the residual appears to follow a straight line. No evidence of nonnormality or skewness unidentified variable or no potential outlier is located in the normal probability plot.

(ii) Residual versus Fitted Values. If the model is correct and if the assumptions are satisfied, the residual should be structureless; that is, they should be unrelated to any variable including the predicted response or fitted values. It indicates whether the variance is constant, a nonlinear relationship exists, or any outliers exist in the data. This plot should not reveal any unusual pattern. Based on this plot, Figure 7, there is no unusual structure apparently, that is, no obvious pattern. The residual appears to be randomly scattered about the zero line. There is no evidence of nonconstant variance, missing terms, outliers, or any influential points.

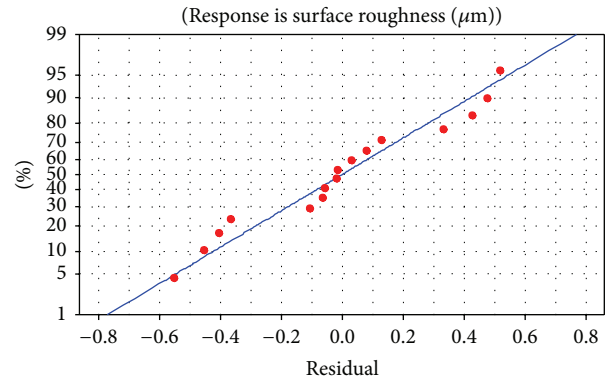

Figure 6: Normal probability plot of residual values.

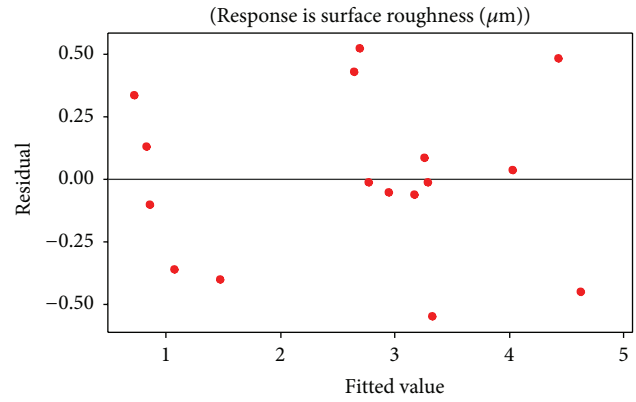

Figure 7: Residual values versus fitted values for surface roughness.

(iii) Standardized Residual versus the Variables. A rough check for outliers is made by examining the standardized residuals. The standardized residuals should be approximately normal with zero mean and unit variance. Thus about 68% of the standardized residuals should fall within the limits ±1, about 95% should fall within ±2, and all of them should fall within ±3. A residual bigger than 3 or 4 standard deviation from zero is a potential outlier. Figures 8, 9, 10, and 11 show the residual versus variables, that is, cutting speed, feed, depth of cut, and approach angle.

(iv) Residual versus Observation Order. This plot is useful when the order of the observations may influence the results, which can occur when the data are collected in a time sequence or in some other sequence. This plot indicates whether there is any correlation between error terms that are near each other. Correlation among residuals may be signified by ascending or descending trends in the residuals and rapid change in sign of the adjacent residuals. Figure 12 almost indicates a fairly satisfactory result.

(v) Interpretation of Plots. The main effect plot for surface roughness is shown in Figure 13; the slopes for feed, DOC, and approach angle are upward (positive); this graph plots the mean of the high and low of each factor. From this graph, it is seen that if the feed, depth of cut, and approach angle increase the surface roughness increases whereas the cutting speed has

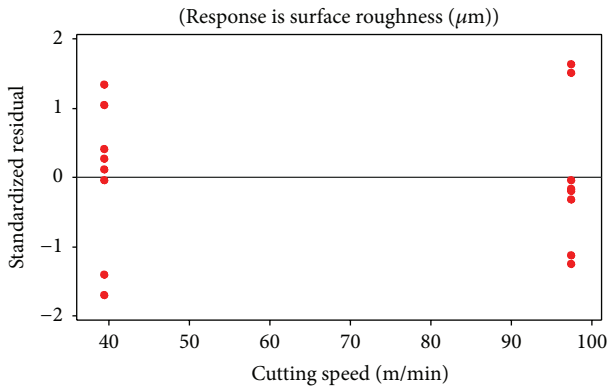

Figure 8: Residual versus cutting speed (m/min).

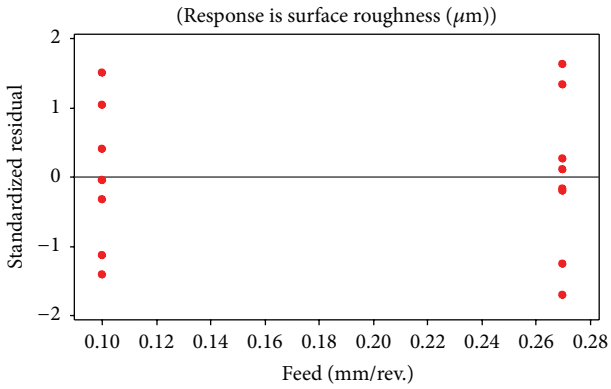

Figure 9: Residual versus feed (mm/rev.).

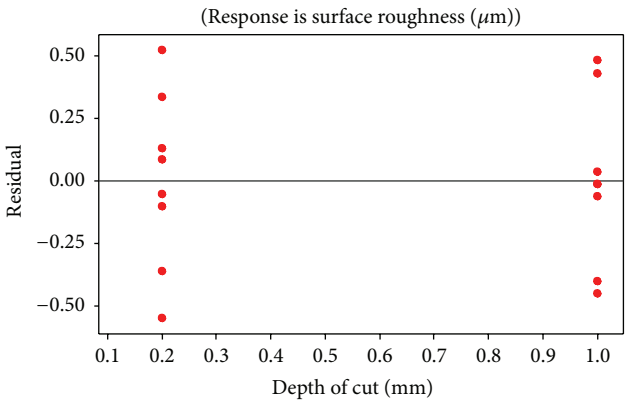

Figure 10: Residual versus depth of cut (mm).

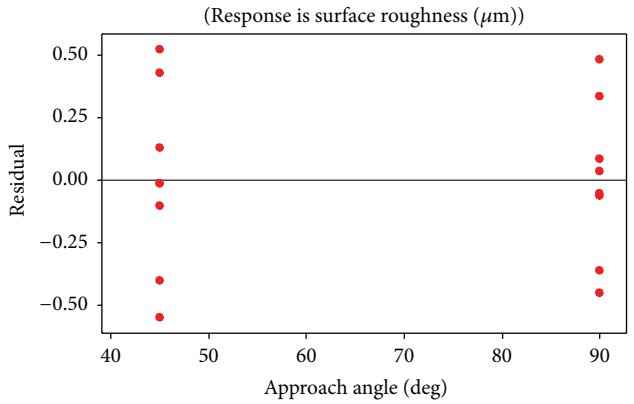

Figure 11: Residual versus approach angle (degree).

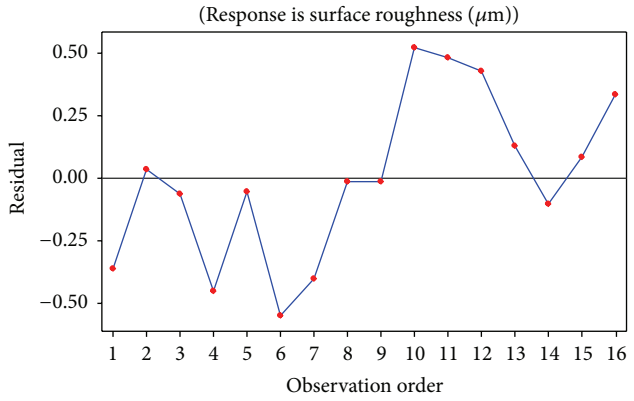

Figure 12: Residual versus observation order.

negligible effect on surface roughness. The main effect plot for main cutting force is shown in Figure 14. From this graph, it is seen that if the feed and depth of cut are increased, the main cutting force also increases whereas cutting speed and approach angle have no effect on main cutting force. Results of interaction plots for surface roughness values are shown in Figure 15. In the plots, the x-axis indicates the value of each parameter at two levels and y-axis the response value. The lines that are nearly parallel, that is, approach angle and feed, cutting speed and approach angle, and so forth, have no interaction whereas there is clear interaction between feed and DOC. Results of interaction plots for main cutting force values are presented in Figure 16. The lines that are nearly parallel indicate that there is no interaction, for example, feed and cutting speed, cutting speed and DOC, approach angle and feed, and cutting speed and approach angle.

With increase in feed the surface roughness increases as expected. It is a well-known theory that, for a given tool nose radius, the theoretical surface roughness $\{R_a \cong f^2/(32 \times \text{nose radius})\}$ is mainly a function of feed. Increase in feed increases the helicoid furrows generated due to the resultant nose shape helicoid tool-work-piece movement. Deeper and broader furrows are formed due to increase in feed resulting in poor R_a values. Also with the increase in feed the contact area between the cutting tool and work material increases and hence the main cutting force increases due to increase in chip load. As the depth of cut increases, the material removal rate increases and therefore there is an increase in main cutting force. On the other hand increase in depth of cut causes increase in the ploughing action of the annealed steel during machining, thereby decreasing the surface roughness. The approach angle along with the nose radius of the tool affects the chip formation in a way that the chip cross section changes. The chip thickness is reduced and the width increases with smaller angle; that is, at larger approach angle the chip thickness increases, which then has a

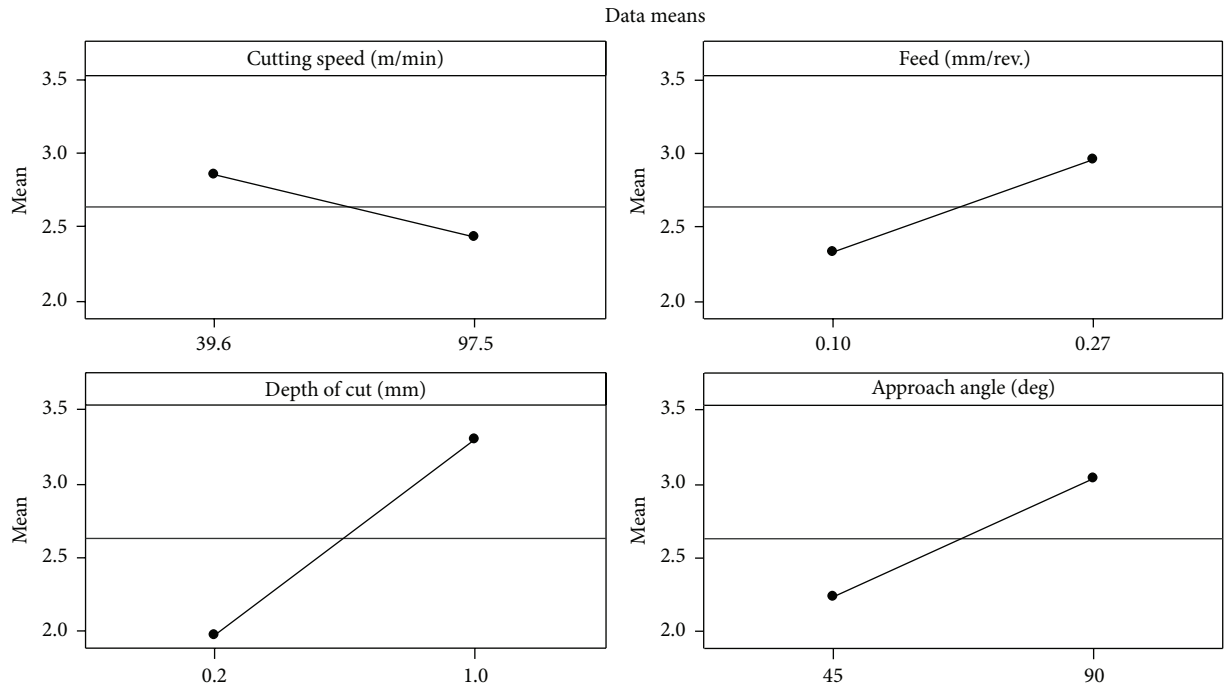

Figure 13: Main effect plot (surface roughness).

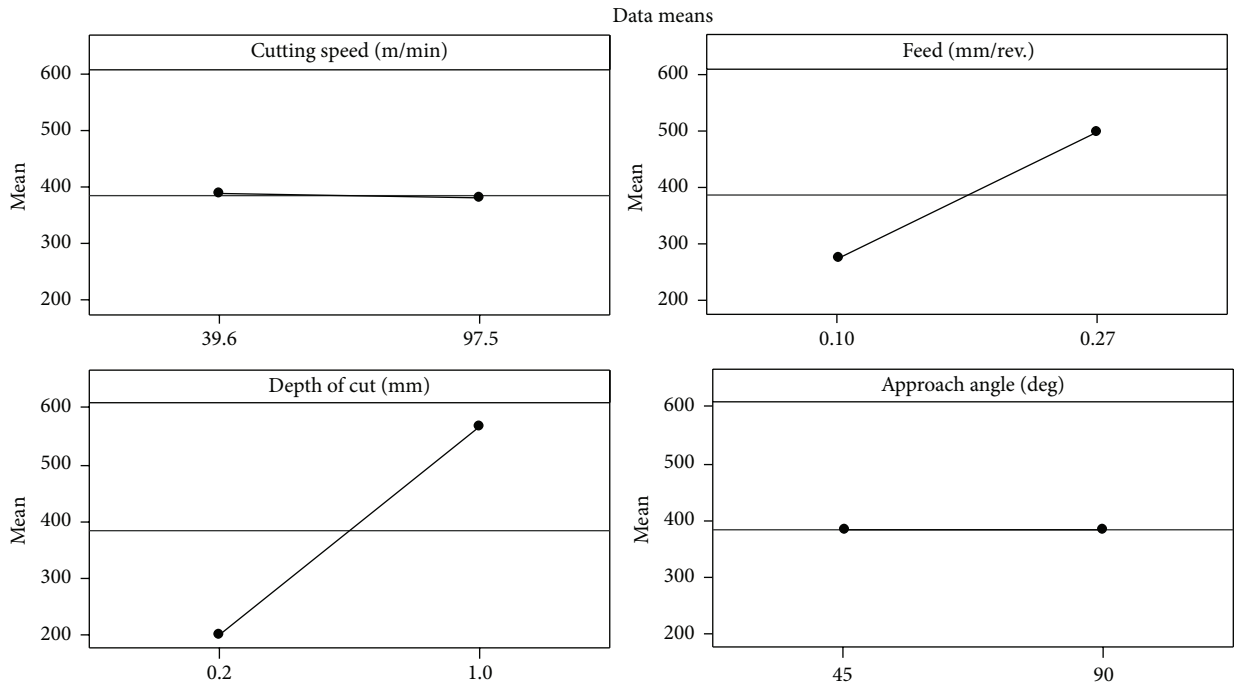

Figure 14: Main effect plot (main cutting force).

negative influence on the machining process, and the surface roughness deteriorates.

3.2. Confirmation Experiments. In order to verify the accuracy of the model developed representing (3) and (4), three confirmation run experiments were performed (Table 10). The test conditions for the confirmation test were so chosen that they are within the range of the levels defined previously [20]. The predicted values and the associated experimental values were compared. The error percentage is within the permissible limits. So, the response equation for the surface roughness and main cutting forces predicted through

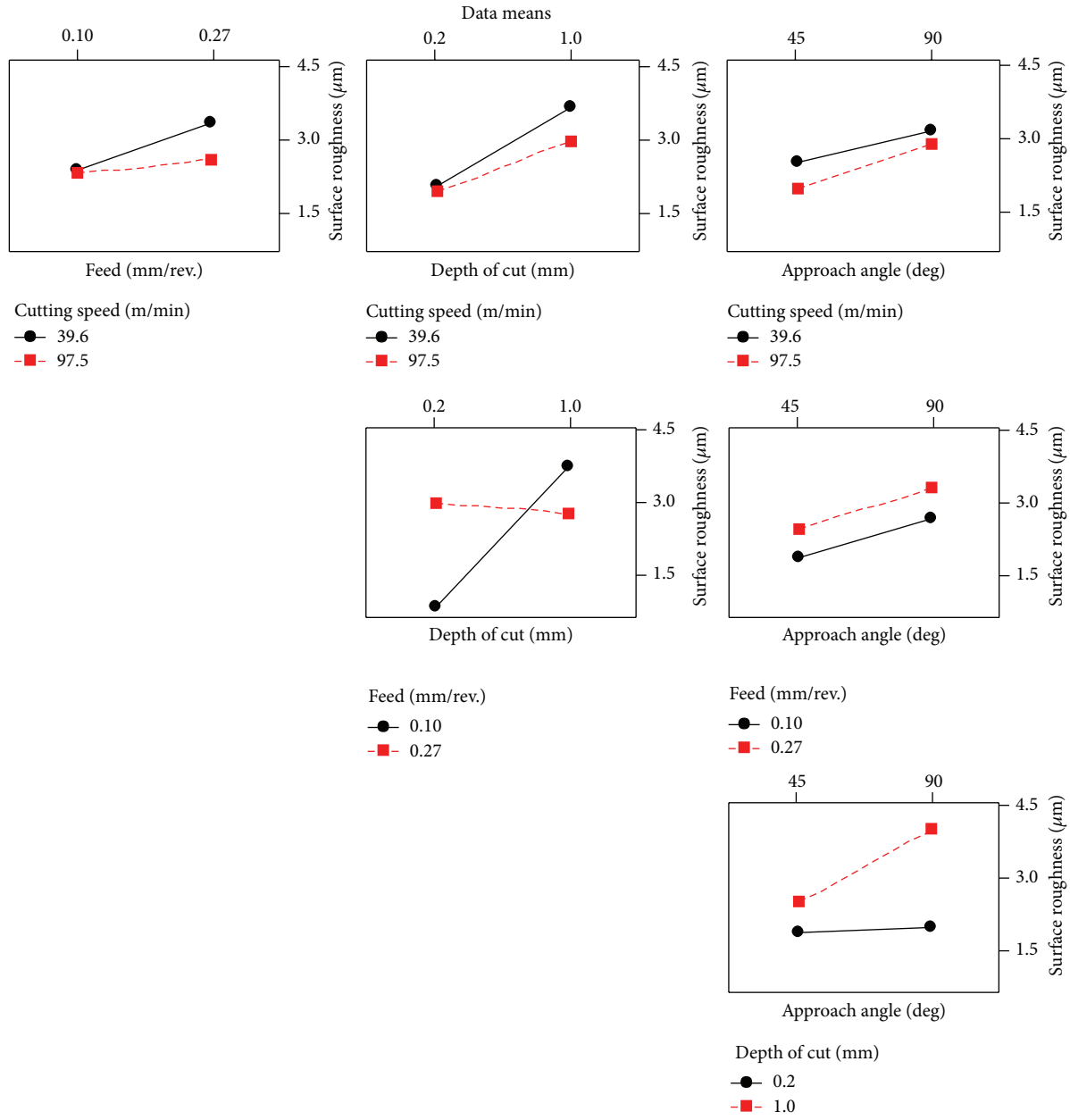

Figure 15: Interaction plots (surface roughness).

Table 10: Confirmation test.

Serial number	"V" (m/min)	"f" (mm/rev.)	"d" (mm)	A_e (degree)	Exp. (R_a)	Pred. (R_a)	Error (%)	Exp. (F_c)	Pred. (F_c)	Error (%)
1	58.4	0.13	0.4	45	2.97	3.18	7.07	496	462	6.8
2	72.7	0.18	0.6	75	3.23	3.48	7.7	492	519	5.4
3	97.5	0.21	0.8	90	3.53	3.67	3.6	544	582	6.9

this model can be used to successfully predict the surface roughness and main cutting force for any combination of the cutting speed, feed, depth of cut, and approach angle within the range of the experimentation performed.

Table 10 presents the results between experimental run and predicted data for surface roughness and main cutting force. It is found that the difference between the experimental value and predicted model is very small. The difference in

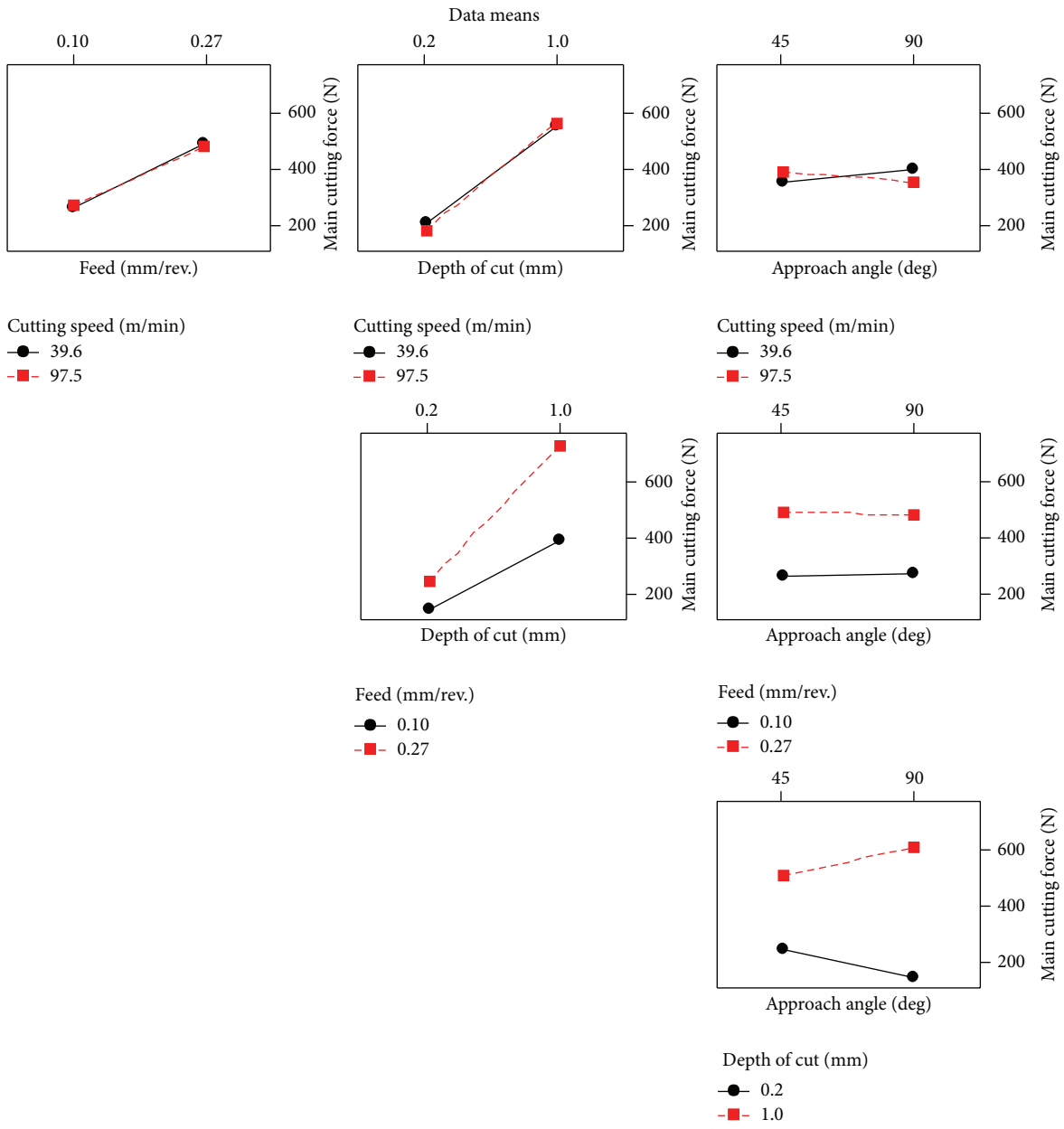

Figure 16: Interaction plots (main cutting force).

terms of error is less than 7.7% for surface roughness and less than 6.9% for main cutting force. It proves that the model and equation generated give a fair reading indicating a reasonable model as per the previous study by Lazoglu et al. [21]. The results obtained also validated the reliability of the model.

4. Conclusion

The commercial value of a material is due to its properties. AISI D6 tool steel can be commercially exploited and used in several industrial applications because of the following reasons:

(1) 2.130% of carbon presence along with other alloying elements in this steel is an added advantage but the long granular carbides formed after heat treatment, if found on the machined surface, are prone to cracks on sudden loads. Therefore, this steel can be used for industrial dies and tools like form rolls, thread rolls, and gauges which are not subjected to any sudden impact loads.

(2) The tensile strength of the hardened steel improved phenomenally from 687.90 to 1855.03 N/mm^2 and the ductility decreased from 7.40 to 1.16%. Although compressive yield strength is of more importance, tensile strength and ductility are important properties in tooling area as in some situations a preexisting crack in tools starts developing due to tension. No yielding phenomenon was observed in the hardened

specimen and fracture occurred without any prior yield. The yield strength of the annealed steel was 445.69 N/mm^2.

(3) The material has a very poor resistance to impact in both annealed and hardened condition. The puzzling observation is no change in toughness after hardening and tempering suggesting that the toughness of the steel in annealed state is terribly low and hence has limited applications as compared to other direct hardening tool steels. Therefore, in certain industrial applications like thread rolls, which are not subjected to heavy impacts, gradual loads are applied on the blank, and the tool steel can be used as thread rolls. Hence an appropriate toughness is sufficient if handled with care. Due to its favourable property profile, the tool steel is capable of performing as thread rolls for threading low strength threaded components (mild steel) in an economical manner. Similar tools like extrusion dies for tube forming or gauges for measurements can be manufactured with the help of this tool steel.

(4) Linear regression model is a good fit for both main cutting force and surface roughness measured during machining of annealed steel. The DOC is the most significant factor followed by feed for main cutting force and surface roughness. If the feed, depth of cut, and approach angle increase, the surface roughness increases whereas the cutting speed has negligible effect on surface roughness. If the feed and depth of cut are increased, the main cutting force also increases whereas cutting speed and approach angle have no effect on main cutting force.

(5) Verification experiments carried out show that the empirical models developed can be used for turning of annealed AISI D6 steel within the error of 8%.

Conflict of Interests

The authors declare that there is no conflict of interests regarding the publication of this paper.

References

[1] B. Podgornik, F. Majdic, V. Leskovsek, and J. Vizintin, "Improving tribological properties of tool steels through combination of deep-cryogenic treatment and plasma nitriding," *Wear*, vol. 288, pp. 88–93, 2012.

[2] M. C. Shaw, *Work Material Consideration, Metal Cutting Principles*, Oxford University Press, Oxford, UK, 2nd edition, 2005.

[3] K. Amini, S. Nategh, and A. Shafyei, "Influence of different cryotreatments on tribological behavior of 80CrMo12 5 cold work tool steel," *Materials and Design*, vol. 31, no. 10, pp. 4666–4675, 2010.

[4] R. N. Naravade, U. N. Gujar, and R. R. Kharde, "Optimization of cryogenic treatment on wear behaviour of AISI D6 tool steel by using DOE/RSM," *International Journal of Engineering and Advanced Technology*, vol. 2, no. 2, pp. 239–244, 2012.

[5] J. D. Bressan, D. Kohls, and A. Tramontin, *Fracture Toughness of AISI D6 Tool Steel As Received and with Heat Treatment*, UDESCO, São Paulo, Brazil, 2013.

[6] J. P. Davim and L. Figueira, "Machinability evaluation in hard turning of cold work tool steel (D2) with ceramic tools using statistical techniques," *Materials and Design*, vol. 28, no. 4, pp. 1186–1191, 2007.

[7] M. C. Cakir, C. Ensarioglu, and I. Demirayak, "Mathematical modeling of surface roughness for evaluating the effects of cutting parameters and coating material," *Journal of Materials Processing Technology*, vol. 209, no. 1, pp. 102–109, 2009.

[8] B. Fnides, M. A. Yallese, T. Mabrouki, and J. F. Rigal, "Application of RSM for determining cutting force model in turning hardened AISI H11 hot work tool steel," *Indian Academy of Sciences*, vol. 36, no. 1, pp. 109–203, 2011.

[9] K. Bouacha, M. A. Yallese, T. Mabrouki, and J.-F. Rigal, "Statistical analysis of surface roughness and cutting forces using response surface methodology in hard turning of AISI 52100 bearing steel with CBN tool," *International Journal of Refractory Metals and Hard Materials*, vol. 28, no. 3, pp. 349–361, 2010.

[10] J. G. Lima, R. F. Ávila, A. M. Abrão, M. Faustino, and J. P. Davim, "Hard turning: AISI 4340 high strength low alloy steel and AISI D2 cold work tool steel," *Journal of Materials Processing Technology*, vol. 169, no. 3, pp. 388–395, 2005.

[11] D. I. Lalwani, N. K. Mehta, and P. K. Jain, "Experimental investigations of cutting parameters influence on cutting forces and surface roughness in finish hard turning of MDN250 steel," *Journal of Materials Processing Technology*, vol. 206, no. 1–3, pp. 167–179, 2008.

[12] A. Ebrahimi and M. M. Moshksar, "Evaluation of machinability in turning of microalloyed and quenched-tempered steels: tool wear, statistical analysis, chip morphology," *Journal of Materials Processing Technology*, vol. 209, no. 2, pp. 910–921, 2009.

[13] ASM International, *ASM Handbook Volume 9: Metallography and Microstructures*, ASM International, Metals Park, Ohio, USA, 10th edition, 1990.

[14] ASM International, *ASM Handbook Volume 1: Properties and Selection: Nonferrous Alloys and Special Purpose Materials*, ASM International, Metals Park, Ohio, USA, 10th edition, 1990.

[15] Bureau of Indian Standard, "Methods for rockwell hardness test for metallic material," IS 1586-2000, Bureau of Indian Standard, New Delhi, India, 1994.

[16] Bureau of Indian Standard, *IS: 1501-2002 'Methods for Vicker Hardness Test for Metallic Material'*, Bureau of Indian Standard (BIS), New Delhi, India, 3rd edition, 1997.

[17] Bureau of Indian Standard, "Metallic material, tensile testing at ambient temperature," Tech. Rep. IS: 1608-2005, BIS, New Delhi, India, 1997, 3rd revision.

[18] Bureau of Indian Standard, "Method for charpy impact test (V-notch) on metallic material," IS 1757-1988, Bureau of Indian Standard, New Delhi, India, 1989.

[19] D. C. Montogomery, *Two-Level Factorial Design, Design and Analysis of Experiments*, John Wiley & Sons, 7th edition, 2009.

[20] A. J. Makadia and J. I. Nanavati, "Optimisation of machining parameters for turning operations based on response surface methodology," *Measurement: Journal of the International Measurement Confederation*, vol. 46, no. 4, pp. 1521–1529, 2013.

[21] I. Lazoglu, K. Buyukhatipoglu, H. Kratz, and F. Klocke, "Forces and temperatures in hard turning," *Machining Science and Technology*, vol. 10, no. 2, pp. 157–179, 2006.